Spontaneous hair follicle germ (HFG) formation *in vitro*, enabling the large-scale production of HFGs for regenerative medicine

CrossMark

Tatsuto Kageyama [a], Chisa Yoshimura [a], Dina Myasnikova [a], Ken Kataoka [b], Tadashi Nittami [a], Shoji Maruo [a], Junji Fukuda [a, *]

[a] Faculty of Engineering, Yokohama National University, 79-5 Tokiwadai, Hodogaya-ku, Yokohama, Kanagawa 240-8501, Japan
[b] Biomedical Engineering, Okayama University of Science, 1-1 Ridai-chou, Kita-ku, Okayama, Okayama 700-0005, Japan

ARTICLE INFO

ABSTRACT

Hair follicle morphogenesis is triggered by reciprocal interactions between hair follicle germ (HFG) epithelial and mesenchymal layers. Here, we developed a method for large-scale preparation of HFGs *in vitro* via self-organization of cells. We mixed mouse epidermal and mouse/human mesenchymal cells in suspension and seeded them in microwells of a custom-designed array plate. Over a 3-day culture period, cells initially formed a randomly distributed single cell aggregate and then spatially separated from each other, exhibiting typical HFG morphological features. These self-sorted hair follicle germs (ssHFGs) were shown to be capable of efficient hair-follicle and shaft generation upon intracutaneous transplantation into the backs of nude mice. This finding facilitated the large-scale preparation of approximately 5000 ssHFGs in a microwell-array chip made of oxygen-permeable silicone. We demonstrated that the integrity of the oxygen supply through the bottom of the silicone chip was crucial to enabling both ssHFG formation and subsequent hair shaft generation. Finally, spatially aligned ssHFGs on the chip were encapsulated into a hydrogel and simultaneously transplanted into the back skin of nude mice to preserve their intervening spaces, resulting in spatially aligned hair follicle generation. This simple ssHFG preparation approach is a promising strategy for improving current hair-regenerative medicine techniques.

© 2017 Elsevier Ltd. All rights reserved.

1. Introduction

Hair loss is a common disorder that affects men, women, and children in response to various factors, including age, disease, and medical treatment. In fact, approximately 50% of men and 25% of women worldwide experience partial hair loss by the age of 50 years [1]. The current treatment for severe hair loss conditions, such as androgenic alopecia, predominantly relies on translocation of a patient's remaining hair follicles to alopecic areas [2]. However, this approach is limited to cases in which adequate autologous hair follicles are available. The hypothesis that hair follicles can be reconstituted from dissociated and expanded hair follicle-derived stem cells has thus been explored, based on our current understanding of hair follicle development *in vivo* [3,4]. During embryonic development, reciprocal interactions between epithelial and mesenchymal germ layers stimulate hair follicle morphogenesis

[5,6]. Many researchers have attempted to recapitulate these interactions *in vitro* using a range of different strategies and approaches [4,7,8]. Successful hair-follicle regeneration via cotransplantation of epithelial and mesenchymal cell populations in a mixed cell suspension has been possible for the last few decades [9–12]. While these cells spontaneously organize themselves at transplantation sites and replicate the anatomical features and positions observed to occur in *in vivo* [9–12], the efficiency of hair generation has been limited probably due to insufficiency of epithelial-mesenchymal interactions [4].

Recent studies have shown that hair generation efficiency can be improved by fabricating a mesenchymal-cell aggregate and transplanting this aggregate with or without epithelial cells [13–17]. An even higher level of efficiency was more recently achieved using a sophisticated organ-germ culture approach, in which epithelial and mesenchymal cell pellets were separately prepared via centrifugation and then merged to provoke epithelial-mesenchymal interactions just prior to transplantation [18]. These compartmentalized aggregates, named bioengineered HFGs, were

shown to induce the regeneration of functional hair follicles and of associated host tissues and characteristics, including the arrector pili muscle, nerve fibers, and repeated hair cycles. This technique represents a promising new approach to hair regenerative medicine. However, it is currently limited by the need to manually prepare the bioengineered HFGs under a microscope. This labor-intensive task is impractical given that treating a single human patient may require hundreds of thousands of hair follicles.

Thus, in the present study, we developed a simple and practical method for simultaneously preparing a large number of HFGs. A key finding of the present study was that, while epithelial and mesenchymal cell populations initially formed a mixed single aggregate, they subsequently spontaneously separated from each other inside the aggregate and adopted a compartmentalized, HFG-like morphology during the subsequent 3 days of culture. We examined whether these self-sorted HFGs (ssHFGs) were able to generate hair follicles in vivo and subsequently attempted large-scale preparation of ssHFGs via this novel self-organization technique using a custom-designed microwell array 'HFG chip'. Finally, we investigated the effects of modulating the oxygen supply to the HFG chip on the ability of the HFGs to self-organize and generate hair follicles in vivo.

2. Materials and methods

2.1. Materials and reagents

The materials utilized for HFG chip fabrication included cyclo-olefin plates (ZEONOR; Zeon, Japan), epoxy resin (Nissin Resin, Japan), polydimethylsiloxane (PDMS) prepolymer solution and curing agent (Shin-etsu Silicone, Japan), and φ6-cm cell culture dishes (TPP, Japan).

The reagents utilized used for cell isolation, culture, and analysis included 35-mm cell strainer mesh (BD Biosciences), phosphate-buffered saline (PBS), trypsin, penicillin-streptomycin mixed solution, Vybrant DiI cell-labeling solution, 1% bovine serum albumin (BSA), Triton X-100 (Invitrogen, Carlsbad, CA, USA), dispase II, collagenase type I, ethidium bromide, 4% formaldehyde in PBS, Bouin solution, 10% formaldehyde neutral buffer solution, t-butyl alcohol (Wako Chemicals, Japan), non-cell-adhesive round-bottom 96-well 'Prime surface 96 U' plates (Sumitomo Bakelite, Japan), epidermal keratinocyte growth medium-2 (KG2; Kurabo, Japan), Dulbecco's modified Eagle's medium (DMEM), fetal bovine serum (FBS), 25% glutaraldehyde, fast blue RR salt, 3-hydroxy-N-(3-nitrophenyl)-2-naphthamide (Naphthol AS-BS), 4,6-diamino-2-phenylindole (DAPI; Sigma, St. Louis, Mo, USA), and rhodamine-phalloidin (Cytoskeleton, USA). The antibodies used in this study included rabbit anti-versican (Millipore), rabbit anti-vimentin, rabbit anti-cytokeratin 15 (K15), rat anti-CD34 (Abcam, Cambridge, UK), rabbit anti-N-cadherin (Thermo Fisher), and rabbit anti-hypoxia-inducible factor (HIF) 1α (Sigma) antibodies, as well as goat anti-rabbit IgG (H+L) Alexa Fluor 488, goat anti-rat IgG (H+L) Alexa Fluor 488, and goat anti-rabbit IgG (H+L) Alexa Fluor 555 highly cross-absorbed secondary antibodies (Invitrogen). Unless otherwise indicated, all other chemicals were purchased from Wako Chemicals.

2.2. Animals

Pregnant C57BL/6 and 5-week-old ICR nude mice were purchased from CLEA (Japan) and Charles River (Japan), respectively. All mouse care and handling was conducted in strict accordance with the requirements of the Animal Care and Use Committee of Yokohama National University.

2.3. Preparation of mouse epithelial and mesenchymal cells

Embryonic mice (E18) were resected from a C57BL/6 pregnant mouse, and small pieces of their back skin were then harvested under a surgical microscope. After being aseptically treated with 4.8 U/mL dispase II (60 min), the epithelial and mesenchymal layers of these skin samples were separated using tweezers [19]. The epithelial layer was treated with 100 U/mL collagenase type I (2 × 40 min), and 0.25% trypsin (10 min) at 37 °C. The dermal layer was treated only with 100 U/ml collagenase type I (2 × 40 min) at 37 °C. Debris and undissociated tissues were removed using a cell strainer. After centrifugation (1000 rpm, 3 min), the epithelial and mesenchymal cells were resuspended in DMEM or KG2, respectively, and counted. The two cell types were then mixed and cocultured in a mixed 'DMEM/KG2' culture medium that comprised DMEM and KG2 (1:1 ratio), supplemented with 10% FBS and 1% penicillin-streptomycin.

2.4. Spontaneous ssHFG formation

Mouse embryonic epithelial and Vybrant DiI-labeled mesenchymal cells were separately suspended at a series of densities (0.5, 1, 2, 4, 8, 16, or 32×10^3 cells/0.1 mL) in DMEM/KG2 culture medium. An epithelial cell suspension and a mesenchymal cell suspension (of equal density) were then mixed and seeded in one well of a non-cell-adhesive round-bottom 96-well plate. After 3 days of culture, the resulting ssHFGs were fixed with 4% formaldehyde in PBS, stained with DAPI, and observed using a confocal laser-scanning microscope (LSM 700; Carl Zeiss, Germany) and a fluorescent microscope (DP-71; Olympus, Japan). In order to analyze their alkaline phosphatase (ALP) activity, the HFGs were fixed (30 s) with 60% citrate-buffered acetone, washed with MilliQ water, and stained for 30 min at room temperature with ALP dye (4% Naphthol AS-BS solution diluted with Fast blue RR salt solution), according to the manufacturer's instructions. The stained ssHFGs were then observed using a digital microscope (VHX-1000; Keyence, Japan). In order to observe their fine structures, the ssHFGs on the chip were also imaged using scanning electron microscopy (SEM; Miniscope, Hitachi, Japan). To prepare samples for SEM, the ssHFGs were washed with PBS, fixed for 1 h with a mixed solution of 2.5% glutaraldehyde and 2% formaldehyde in PBS, washed again with PBS, and dehydrated via a 30–90% ethanol gradient, before being washed three times with absolute ethanol. This final solution was then substituted with 100% t-butyl alcohol, and the ssHFGs were cooled at 4 °C for 1 h and −20 °C 1 h. The ssHFGs were finally lyophilized, and SEM images were taken at 5–10 kV.

2.5. Inhibition of ssHFG formation

The ability of the epithelial/mesenchymal cells to self-organize to form HFGs was evaluated in the presence of the cell-sorting inhibitor Y-27632 [20]. Mouse epithelial and Vybrant DiI-labeled mesenchymal cells were suspended in culture medium (4×10^3 cells/mL of each cell type) containing 30 μM Y-27632 and were seeded into a 96-well plate. After 3 days of culture, the spatial distribution of the cells was observed using a fluorescent microscope, and the relative expression levels of genes associated with hair follicle morphogenesis were evaluated via real-time reverse transcription polymerase chain reaction (RT-PCR) analysis. The achieved hair generation efficiency (i.e., the proportion of total transplantation sites observed to exhibit hair generation) was then examined via the intracutaneous transplantation of ssHFGs into nude mice.

2.6. Intracutaneous transplantation of ssHFGs

Under anesthesia, ssHFGs were transplanted into shallow stab wounds prepared on the backs of nude mice using a 20-G ophthalmic V-lance (Alcon, Japan), before the transplantation sites were rubbed with ointment. The mice were housed under pathogen-free conditions with feeding *ad libitum* for up to 10 weeks. Transplanted sites were observed every 2–3 days, and images of generated hairs were taken using a digital microscope (VHX-1000; Keyence) and digital camera (Tough, Olympus, Japan). Hematoxylin-eosin (HE) and immunohistochemical (versican and CD34) staining was performed to characterize hair follicle stem cells 18 days after transplantation. Cuticles of generated hairs were observed via SEM at 5–10 kV.

2.7. HFG chip fabrication

The HFG chip was fabricated via micro-milling and molding processes (Fig. 1A). Briefly, microwell array configurations (diameter, 1 mm; pitch, 1.3 mm; depth, 500 μm) in a 20×20 mm region were designed using CAD/CAM software (Vcave pro; Vectric Co., UK), and the resulting data were sent to a computer-aided micro-milling machine (MDX-540; Roland, Japan) to fabricate a negative-mold from a polyolefin plate. Epoxy resin was poured onto this negative mold and cured (24 h, room temperature) to produce a positive mold. A PDMS solution (10:1 mix of a pre-polymer solution and curing agent) was poured onto the positive mold and cured in an oven (3 h, 80 °C). The thickness of the PDMS substrate at the floor of the microwells was set to 1.5 mm by adjusting the volume of the utilized PDMS solution. The surface of the PDMS substrate, including the microwells, was modified via exposure to a 4% pluronic F-127 solution for 6 h to render it non-cell-adhesive. After substantial washing with MilliQ water to remove excess pluronic F-127, the PDMS substrate was used for cell culture.

2.8. Large-scale ssHFG preparation

Cell suspension solutions (2 mL) containing mouse epithelial and mesenchymal cells (0.5 and 1.0×10^6 cells/mL of each cell type) were poured into the HFG chips and incubated (37 °C) in DMEM/ KG-2 medium. After 3 days of culture, cell morphology and function were evaluated via HE staining, RT-PCR, and immunohistochemical analysis, and cell aggregates were intracutaneously transplanted into the back skin of nude mice. All transplanted sites were observed using a digital microscope (VHX-1000; Keyence) and digital camera (Tough; Olympus) for 21 days after
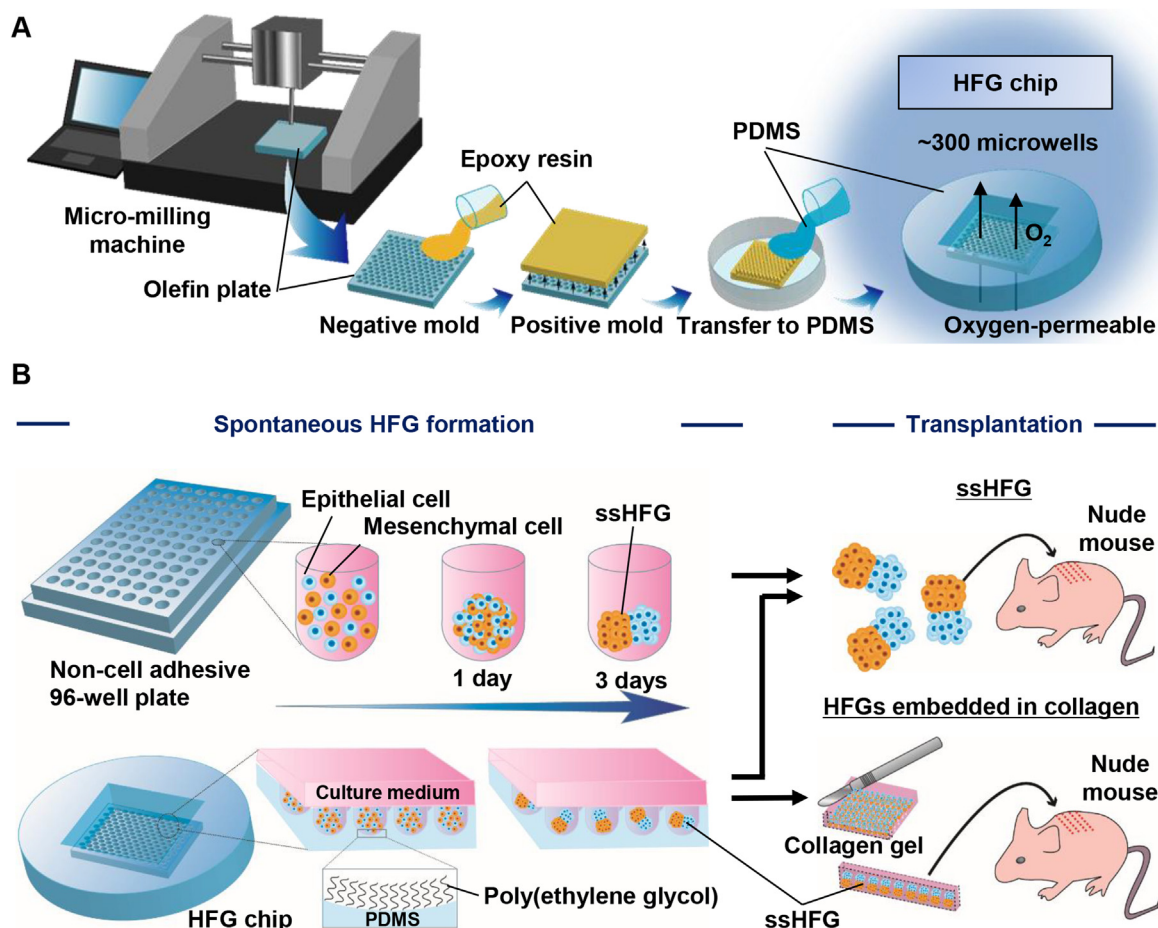

Fig. 1. Schematic representation of a method for the large-scale preparation of self-sorted hair follicle germs (ssHFGs). (A) The HFG chip was fabricated via a two-step molding process. First, an olefin plate was micro-milled to produce a plate with 300 round-bottomed (φ1.0-mm) wells. These milled structures were then transferred to epoxy resin, and the resulting positive mold was covered with polydimethylsiloxane (PDMS) to produce an HFG chip. **(B)** Spontaneous formation and intracutaneous transplantation of ssHFGs. Epithelial and mesenchymal cells were mixed and seeded in a 96-well plate and HFG chip. In both culture vessels, the two cell types formed a randomly distributed aggregate during the first day of culture; however, during the following 3 days of culture, they spatially separated and adopted HFG-specific features. Within the chip, HFG formation was observed to occur in an identical manner in almost all (~300) wells. The generated HFGs were transplanted into mice to evaluate the ability to generate hair follicles.

transplantation. As a comparison, the same experiments were conducted using the typical spheroid-preparation 'hanging drop' approach [21] and/or using HFG chips fabricated with polymethyl methacrylate (PMMA), which had the same number of microwells as those fabricated using PDMS, but almost no oxygen permeability [22].

2.9. Generation of spatially aligned hair follicles

To examine the feasibility of simultaneously transplanting ssHFGs in a spatially aligned manner (Fig. 1B), mouse epithelial and mesenchymal cells (2-mL solution, 2.5×10^5 cells/mL of each cell type) were seeded into a HFG chip and cultured for 3 days. After aspirating the culture medium, 1 mL of type I collagen solution (3.0 mg/mL; Nitta Gelatin, Japan) was poured onto the HFG chip. To aid handling, a mechanical support mesh (Pip, Japan) was placed onto the chip and allowed to integrate into the collagen during the subsequent incubation (40 min, 37 °C). The resulting collagen-gel sheet containing the two-dimensionally aligned ssHFGs was then peeled free of the HFG chip using tweezers. The gel sheet was cut to allow separation of the rows of ssHFGs so that they were able to be separately intracutaneously transplanted into the back skin of nu/nu mice. The transplanted skin was histologically stained after 21 days.

2.10. Gene expression analysis

Total RNA was extracted from samples using an RNeasy mini kit (Qiagen, Netherlands), and cDNA was synthesized via reverse-transcription using a ReverTraAce RT-qPCR kit (Toyobo, Japan), according to the manufacturer's instructions. qPCR was performed using the StepOne Plus RT-PCR system (Applied Biosystems, Foster City, CA, USA), with SYBR Premix Ex Taq II (Takara-bio, Japan), and primers for versican (GACGACTGTCTTGGTGG, ATATCCAAA-CAAGCCTG), Nexin (CCACGCAAAGCCAAGACGAC, GAAACCGGCCTGCTCATCCT), *IGFbp5* (ATGAGACAGGAATCCGAACA, TCAACGTTACTGCTGTCGAA), *TGFβ2* (TCCCGAATAAAAGCGAAGAG,

AAGCTTCGGGATTTATGGTG), *Hey1* (TGTTCCATGTCCCCAACGAC, TGATGTCCGAAGGCACTTCC), *HIF1α* (CAGCTTCCTTCGGACACATAAG, CCACAGCAATGAAACCCTCCA), and *GAPDH* (AGAA-CATCATCCCTGCATCC, TCCACCACCCTGTTGCTGTA) [23,24]. All gene expression levels were normalized to that of *GAPDH*. Relative gene expression was determined using the 2^{-Ct} method and presented as the mean ± standard deviation of four independent experiments. Statistical evaluation of numerical variables was conducted using Student's t-tests, and differences with *p* values of less than 0.05 were considered statistically significant.

2.11. Histological and immunohistochemical staining

For histological staining, samples were washed with PBS and fixed with Bouin solution for 1 h at room temperature. After embedding in a paraffin block, thin (8-μm) sections of each sample were cut and stained with Meyer-hematoxylin and eosin Y solutions.

For immunohistochemical staining, samples were fixed overnight at room temperature with 10% formaldehyde neutral buffer solution, prior to the preparation of frozen (8-μm) sections. The samples were blocked for 1 h at room temperature with a solution containing 1% BSA and 0.01% Triton X-100 in PBS, incubated overnight at 4 °C with the indicated primary antibodies, and then further incubated for 3 h at room temperature with the indicated secondary antibodies in blocking solution. The samples were finally incubated for 8 min in DAPI in PBS, before being visualized and photographed using a confocal laser-scanning microscope (LSM 700; Carl Zeiss).

3. Results and discussion

3.1. Spontaneous ssHFG formation

Mouse embryonic epithelial and mesenchymal cells were observed to spontaneously assemble and to form a single aggregate
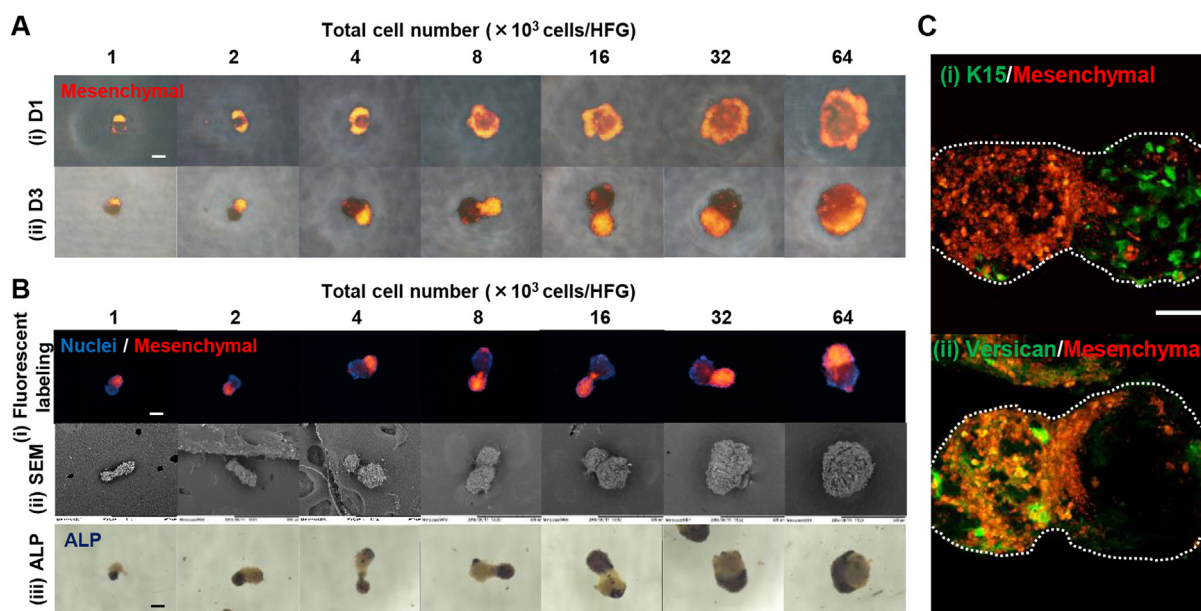

Fig. 2. Spontaneous HFG formation. (A) Changes to the spatial distribution of the two cell types within the single aggregates. Mesenchymal cells were labeled using Vybrant DiI fluorescent dye prior to seeding. By overlaying fluorescent and phase-contrast images of the ssHFGs, the two cell types were confirmed to be homogeneously distributed one day (D1) **(i)** after seeding. However, after 3 days (D3) **(ii)**, they had clearly separated from each other and formed ssHFGs, irrespective of the number of cells ($1-64 \times 10^3$ cells/HFG) included in the original single aggregate. Scale bar: 200 μm. **(B)** ssHFG morphology after 3 days of culture. ssHFGs were visualized via Vybrant DiI counter- (mesenchymal cells) and DAPI staining (both cell types) **(i)**, scanning electron microscopy (SEM) **(ii)**, and alkaline phosphatase (ALP) staining **(iii)**. Scale bar: 200 μm. **(C)** Immunohistochemical counterstaining of ssHFG cross-sections with green fluorescent dye-conjugated antibodies against cytokeratin 15 (K15) **(i)** and versican **(ii)**. Mesenchymal cells are labeled in red by Vybrant DiI. Scale bar: 100 μm. (For interpretation of the references to colour in this figure legend, the reader is referred to the web version of this article.)
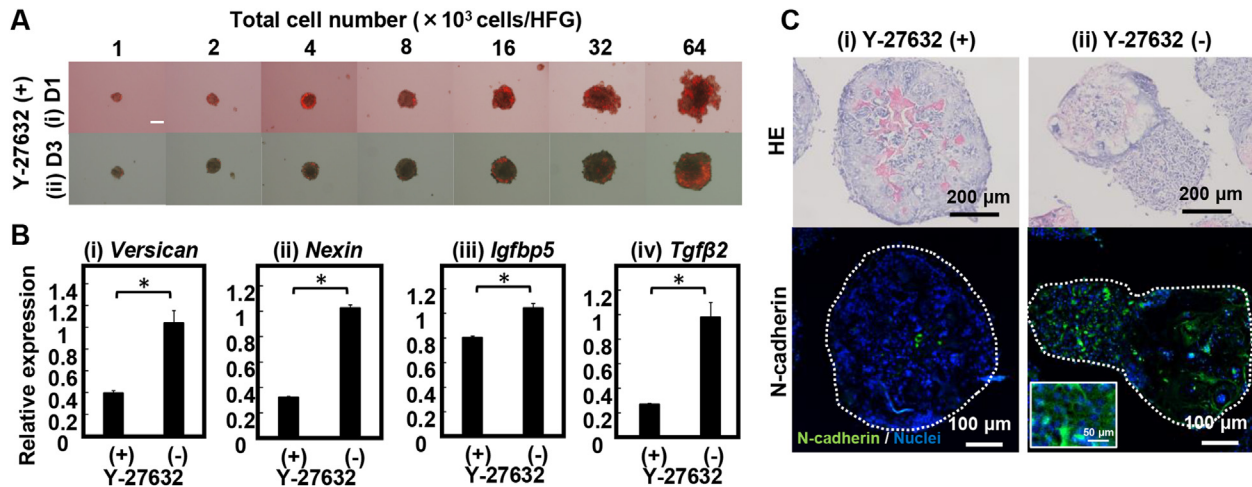
Fig. 3. Effects of cell-sorting inhibition on ssHFG formation. (A) Changes to the spatial distribution of the two cell types within the single aggregates. Mesenchymal cells were labeled using Vybrant DiI prior to seeding, allowing them to be differentiated from epithelial cells in overlaid fluorescent and phase-contrast images. Both cell types were cultured in culture medium containing the ROCK inhibitor Y-27632. The two cell types formed single aggregates after 1 day of culture, irrespective of the number of cells cultured ($1—64 \times 10^3$ cells/HFG). The distribution of the two cell types was homogeneous 1 day after seeding (D1) (i) and remained so, even after 3 days of culture (D3) (ii). Scale bar: 200 μm. (B) Effects of Y-27632 treatment on the expression of genes related to hair induction. Error bars represent the standard deviations calculated from three independent experiments. Numerical variables were statistically evaluated using Student's t-tests (*$p < 0.05$). (C) Cross-sections showing hematoxylin/eosin (HE) and fluorescent staining of ssHFGs treated with (i) or without (ii) Y-27632. The inset indicates a high-magnification image. Blue, cell nuclei; green, N-cadherin. (For interpretation of the references to colour in this figure legend, the reader is referred to the web version of this article.)

in the utilized non-cell-adhesive 96-well plates. The distribution of the two cell types was initially random, however, during the first day of culture, Vybrant DiI-labeled mesenchymal cells gradually migrated toward peripheral portions of the aggregate (Fig. 2A(i), Suppl. Movie 1). Interestingly, the two cell types continued to separate from each other and thereby assumed dumbbell-like configurations after 3 days of culture (Fig. 2A(ii)). These spatial configurations are similar to those previously observed in bioengineered HFGs that were manually prepared by merging pellets comprising the two cell types [18]. Furthermore, the observed spatial separation of the two cell types in the present study occurred, irrespective of the number of cells included in the original single aggregate, although larger ssHFG aggregates tended to adopt spherical rather than dumbbell-like configurations (Fig. 2B(i)). Such spontaneous 'cell sorting' phenomena may be the same as common mechanisms that govern developmental morphogenesis, pattern formation, and tissue homeostasis *in vivo* [7].

Supplementary video related to this article can be found at https://doi.org/10.1016/j.biomaterials.2017.10.056.

SEM imaging of the developing ssHFGs showed them to be composed of dense cell aggregates at both ends of the dumbbell shapes (Fig. 2B(ii)). Enzymatic ALP activity and anti-versican antibody staining, as a known marker of dermal papilla (DP) cells [10] and an extracellular matrix typically produced by DP cells during hair follicle development and anagen-stage growth [23], respectively, were detected in the mesenchymal cell side of the generated ssHFGs (Fig. 2B(iii), 2C(ii)). Conversely, the cytokeratin 15 protein marker of hair-follicle epithelial stem cells [25] was observed only in the epithelial cell side of the ssHFGs (Fig. 2C(i)). These results were consistent with those of previous studies, in which HFGs were manually prepared by merging pellets of the two cell types [18]. The detected DP and epithelial stem cells in the ssHFGs likely played important roles in facilitating the development and/or maintenance of hair follicles and the hair cycle, thereby enabling hair follicle generation after transplantation [26,27].

N- and E-cadherin mediate cell-cell adhesion in mesenchymal and epithelial cells, respectively [28,29]. To evaluate whether either of these cadherin molecules were involved in the mechanisms

underlying the observed spontaneous cell separation during HFG formation, the Y-27632 inhibitor was added to the mixed-cell suspension solution during seeding. Y-27632 is a selective inhibitor of the Rho-associated coiled-coil-containing protein kinase (ROCK), and has been shown to both induce the mesenchymal-epithelial transition and upregulate E-cadherin expression in mesenchymal cells [20,30]. The results of this analysis showed that, in the presence of Y-27632, the two cell types formed single aggregates during the first day of culture (Fig. 3A(i)). However, after 3 days of culture, the two cell types were not completely separated (Fig. 3A(ii)). Although small clusters of mesenchymal cells were observed in the peripheral portions of aggregates, the two cell types were much more widely distributed throughout the aggregates than cells that were not treated with Y-27632 (Fig. 2). Furthermore, the expression levels of genes encoding proteins known to mark hair induction, including versican, nexin, *IGFbp5* (encoding an insulin-like growth factor), and *TGFβ2* (encoding transforming growth factor β2), were downregulated in the presence of Y-27632 (Fig. 3B), likely due to the reduced rate of reciprocal epithelial/mesenchymal cell interactions. Immunostaining to detect N-cadherin in aggregates treated with versus without Y-27632 revealed that N-cadherin-positive cells were predominant in mesenchymal cells and only partially observed in the epithelial cell side of aggregates in the absence of Y-27632 (Fig. 3C(ii)). The cells were in fact virtually absent from aggregates in the presence of Y-27632 (Fig. 3C(i)). These results suggested that Y-27632 downregulated N-cadherin expression in the mesenchymal cells, resulting in disrupting of self-sorting for HFG formation. Thus, spontaneous HFG formation was most likely regulated by cadherin-mediated cell-sorting. Unlike our findings, previous studies showed that keratinocytes and adult DP cells formed a core-shell structure via cell sorting [17]. To explain the mechanisms of cell sorting, the differential adhesion hypothesis was proposed based on thermodynamic principles [31]. The hypothesis states that (i) cell adhesion in multicellular systems depends on energy differences between different types of cells and (ii) an aggregate of cells is motile enough to reach a configuration that minimizes the interfacial energy of the system. Computer simulations based on the hypothesis revealed

that two types of cells with distinct adhesivities formed an aggregate composed of more adhesive cells at the core and less adhesive cells in the outer layer. In contrast, when the adhesivity between heterogeneous cell types was weak compared with those between homogeneous cell types, cells separated from each other in a single aggregate and eventually formed two attached homogeneous aggregates [32]. Thus, both experimental phenomena can be explained by this hypothesis. Aggregates with dumbbell-like configurations may potentially promote hair regeneration because epithelial cyst formation fails in hairs emerging from the skin [18]. We will investigate this phenomenon in our future studies.

3.2. Transplantation of ssHFGs

The ability of the produced ssHFGs to generate hair was examined by grafting them into the back and scalp skins of nude mice after 3 days of culture (Fig. 1B). At 18 days after transplantation, the ssHFGs were found to have generated black hairs at both the back and scalp transplantation sites (Fig. 4A). To examine the effects of cell number on the ability of single ssHFGs to generate hair, we prepared and transplanted ssHFGs comprised of varying cell numbers. The results of this analysis showed that transplanting an increased number of cells resulted in the generation of a greater number of hairs (Fig. 4B and C(i)). Although transplantation of a single ssHFG generated more than one hair shaft, this is not considered a practical drawback because human scalp hairs emerge as closely clustered units consisting of two, three, four, and sometimes even five hairs, comprising a follicular unit [33]. The hair generation efficiency (i.e., the ratio of the number of hair generated sites to the total number of transplanted sites) was also improved by increasing the number of cells within each single ssHFG (Fig. 4C(ii)). A previous study, in which ssHFGs were manually prepared under a microscope, reported a hair generation efficiency of 38% (1.5×10^4 cells/HFG) [18]. In contrast, our approach achieved an increased efficiency (65% ± 15%, 1.6×10^4 cells/ssHFG), likely

because the produced ssHFGs were formed via the same mechanisms known to occur *in vivo* during embryonic development and thus were undamaged by centrifugation and/or other manual operations.

The generated hair follicles were next analyzed via both HE and immunohistochemical staining (Fig. 5A and B). Versican and the hair-follicle epithelial stem cell marker CD34 were observed in the hair papilla and bulge regions of the generated hair follicles, respectively (Fig. 5B). *In vivo*, the hair follicle is a regenerating organ that undergoes a repeated cycle of growth, regression, and rest phases governed by epithelial/mesenchymal interactions [34]. The length of the hair cycle period, which varies with species, body part, and season, is typically 2–6 years for human scalp hairs, and 25 days for mouse hairs [35,36]. The hair follicles generated via transplantation in the present study underwent two cycles of hair shaft growth and removal within a 56-day period and thereby exhibited the typical cycle period for murine hairs (Fig. 5C). Indeed, the cycle was repeated according to this time period for approximately 180 days, representing the complete murine life cycle (n = 1, data not shown). Furthermore, SEM analysis revealed that the generated hair shafts exhibited morphological characteristics (including hair cuticles) comparable to those of natural hairs from C57BL/6 adult mice (Fig. 5D).

To further investigate the role of epithelial cells in hair generation, ssHFGs comprised of only mesenchymal (but not epithelial) cells were generated, and transplanted into the back skin of nude mice. The mesenchymal cells were observed to form single spherical aggregates during 3 days of culture, irrespective of cell number ($1–64 \times 10^3$ total cells/aggregate; Fig. S1A). These aggregates did generate black hairs by 18 days after transplantation (Fig. S1B), but both the number of generated hairs and the hair generation efficiency were reduced compared with those achieved via transplantation of mixed-cell ssHFGs comprised of any cell number (Fig. S1C). Finally, we transplanted mesenchymal/epithelial cell aggregates (8×10^3 total cells/aggregate, 1:1 ratio of
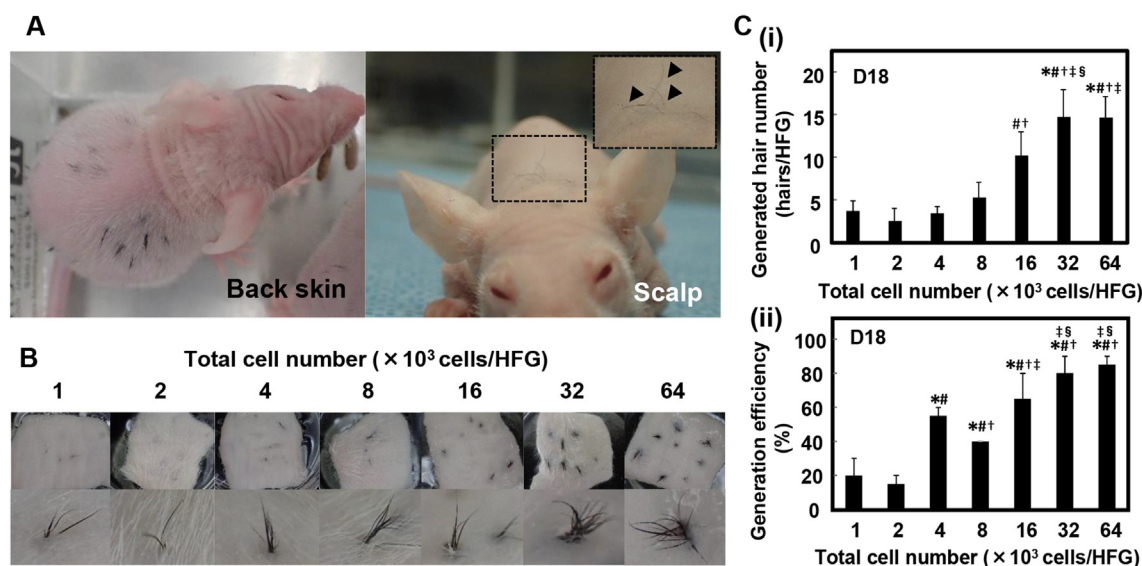

Fig. 4. Hair shaft generation using ssHFGs composed of varying numbers of cells. (A) Hair shafts were observed 18 days after transplantation of ssHFGs (comprising 8×10^3 cells/ HFG) into the back and scalp skin of nude mice. The inset in the right photograph depicts a magnified view of the indicated region. Arrowheads indicate hair shafts. **(B)** Low- and high-magnification stereomicroscopic images of murine back skin 18 days after the transplantation of ssHFGs comprising the indicated number of cells. **(C)** The number of generated hairs **(i)** and generation efficiency achieved **(ii)** 18 days (D18) after transplantation of ssHFGs comprising the indicated number of cells. The generated hair number was defined as the number of hairs generated from one HFG. The generation efficiency was defined as the ratio of the number of hair generated sites to the total number of transplanted sites. For each cell number condition, four independent replicates of 12 ssHFGs were transplanted after 3 days of culture. Error bars represent the standard deviations calculated from three independent experiments. Numerical variables were statistically evaluated using Student-Newman-Keuls tests, where *, #, †, ‡, and § indicate $p < 0.05$ versus 1×10^3, 2×10^3, 4×10^3, 8×10^3, and 16×10^3 cells/HFG, respectively.
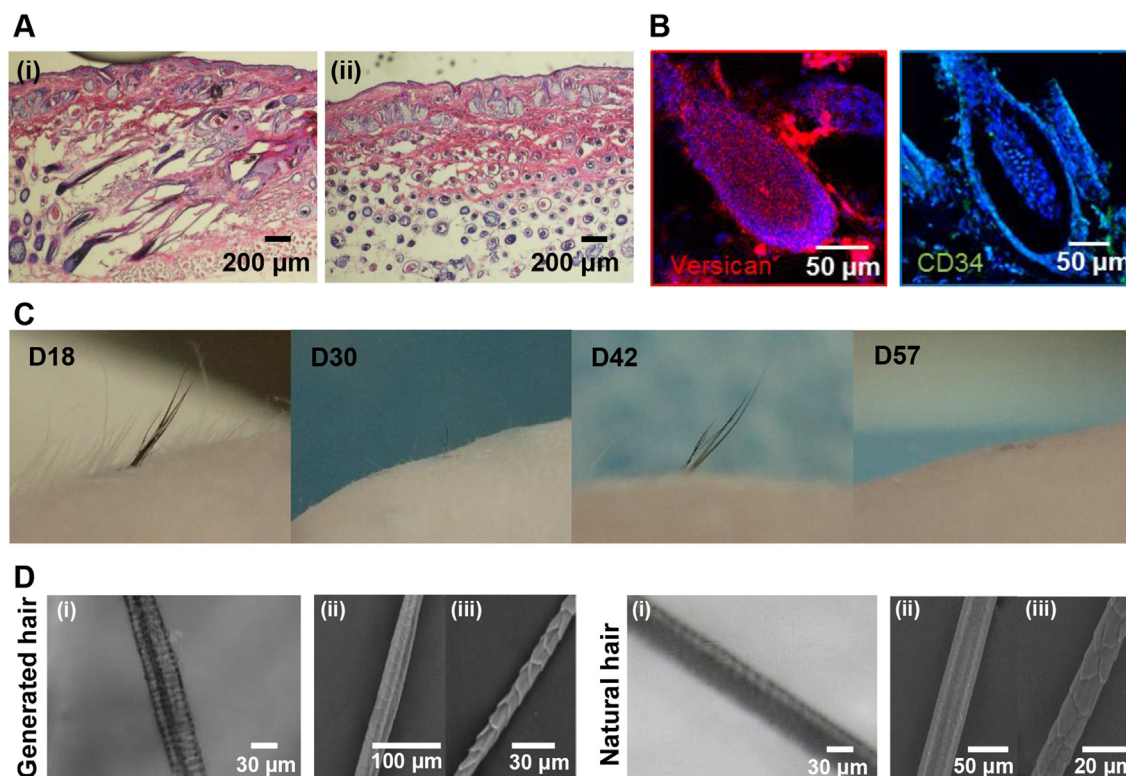
Fig. 5. Morphology of the hairs and composition of the hair cycle generated via ssHFG transplantation. (A) HE staining of skin cross-sections with **(i)** and without **(ii)** ssHFG transplantation. **(B)** Immunohistochemical staining of generated hair follicles. Blue, nuclei; green, CD34; red, versican. **(C)** Composition of generated hair cycle. A specific ssHFG-grafted skin portion was observed for 2 months and photographed on days (D) 18, 30, 42, and 57 after transplantation. **(D)** The morphology of generated and natural hairs was compared via stereo- **(i)** and scanning electron microscopy **(ii, iii)**. (For interpretation of the references to colour in this figure legend, the reader is referred to the web version of this article.)

mesenchymal:epithelial cells), that were either treated or untreated with Y-27632, into the back skin of nude mice. We found that the hair generation efficiency was significantly decreased (by approximately 50%) in the presence versus absence of the inhibitor. These results suggested that spontaneous ssHFG formation by mesenchymal/epithelial cells was crucial to achieve optimal hair generation.

3.3. Microfabrication of the HFG chip for the large-scale preparation of ssHFGs

An HFG chip with ~300 round-shaped microwells (Fig. 6A and B) was fabricated via a two-step molding process (Fig. 1A). A proper oxygen supply is critical for cell growth, particularly when cells form three-dimensional aggregates and when interspaces between aggregates are limited by the need to prepare a large number of aggregates within a discrete space [37]. Since the chip was fabricated using gas-permeable PDMS, it was expected that oxygen would be supplied to the cells via the culture medium from both above and below (i.e., through the PDMS floor of the chip). In fact, PDMS has been estimated to exhibit an oxygen diffusion coefficient and oxygen solubility level 1.5- and 10-fold greater than those exhibited by culture medium (water), respectively [38]. Given that it is also noncytotoxic, transparent, easily able to be sterilized via autoclaving, and well suited to microfabrication, this material has been widely used in various scientific fields to date, e.g., in lab-on-a-chip and tissue engineering approaches [22,39,40].

To characterize the effects of oxygen supply modulation on ssHFG formation and gene expression, we cultured cells on both an oxygen-permeable PDMS HFG chip (oxy(+)), and a chip with the same configuration, but instead fabricated using non-oxygen-permeable PMMA (oxy(−)). Initially, the two seeded cell types aggregated as expected. On the PDMS oxy(+) chip, the cell types separated from each other and formed ssHFGs during the subsequent 3 days of culture (Fig. 6D(i)). In contrast, the cells seeded in the PMMA oxy(−) chip formed poorly delineated aggregates, in which limited or no spatial separation of the two cell types was observed (Fig. 6D(ii)). These results suggested that an adequate oxygen supply was critical for proper ssHFG formation. Nevertheless, at a lower cell density (4×10^3 cells/HFG), ssHFG formation was partially successful, even using the PMMA oxy(−) chip, although the aggregates prepared using the PMMA oxy(−) chip were not able to generate hair when transplanted into nude mice (data not shown).

Next, we further examined the expression levels of *HIF* and the four known hair induction-associated marker genes found to be upregulated on the ssHFGs generated in 96-well plates (Fig. 3B) using cells seeded in oxy(+) and oxy(−) chips at a density of 4×10^3 cells/ssHFG. The results showed that the expression of all four hair induction-associated marker genes was downregulated in cells cultured on the PMMA oxy(−) compared with that of cells cultured on the PDMS oxy(+) chip (Fig. 6E). Conversely, the expression of *HIF-1α*, which is known to mediate cellular responses to hypoxia [38], was twice as high in PMMA oxy(−)- than in PDMS oxy(+)-cultured cells (Fig. 6E). This result was further supported by the observed increase in HIF-1α protein immunostaining of aggregates generated using the PMMA oxy(−) versus the PDMS oxy(+) chips (Fig. 6F).
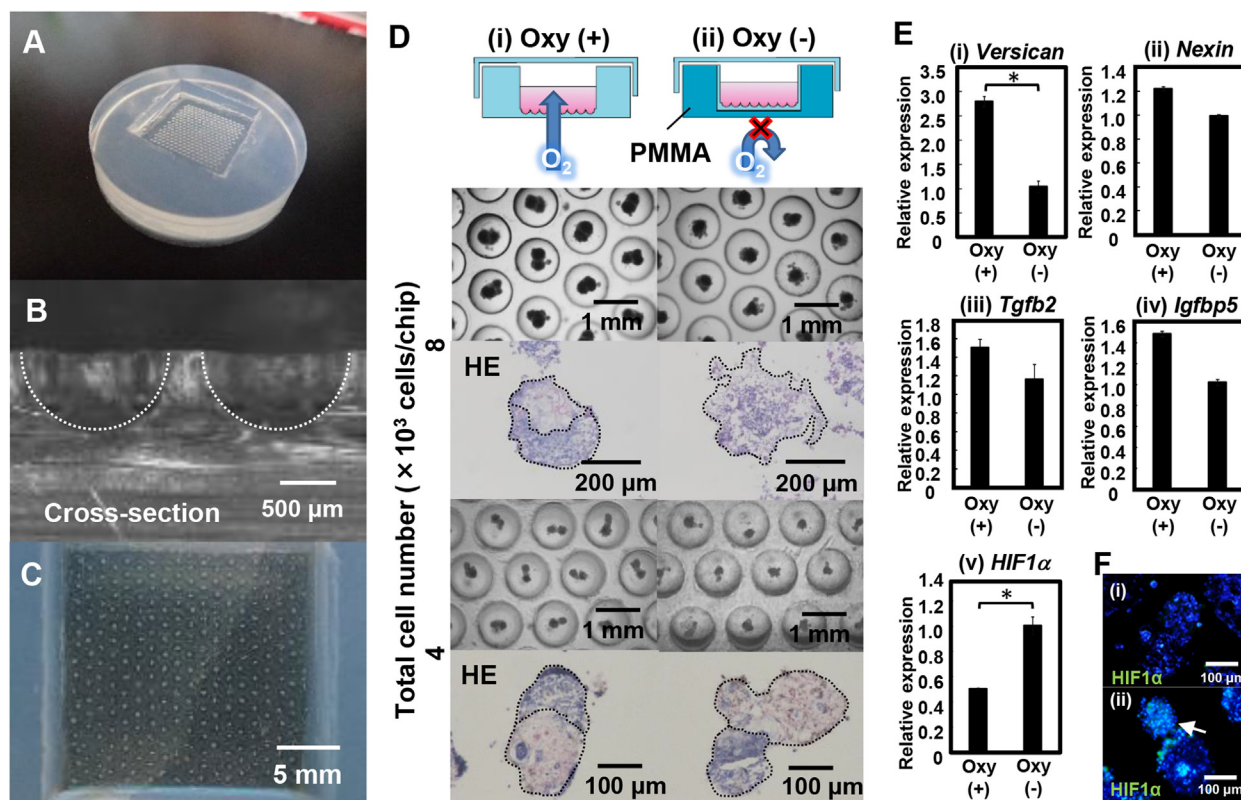
Fig. 6. Use of an HFG chip for the preparation of a large number of ssHFGs. (A) The fabricated HFG chip. **(B)** Cross-section of hemispherical wells in the HFG chip. **(C)** ssHFGs formed in the chip after 3 days of culture. **(D)** Comparisons of HFG chips fabricated using oxygen-permeable PDMS (oxy(+)) and non-oxygen-permeable PMMA (oxy(−)). Epidermal and mesenchymal cells were seeded at 4×10^3 or 8×10^3 total cells/chip on oxy(+) and oxy(−) chips and analyzed via phase-contrast imaging and HE staining after 3 days. **(E)** Expression of hair generation-related genes by cells seeded on oxy(+) and oxy(−) chips, normalized to that of *GAPDH*. Error bars represent the standard deviations calculated from three independent experiments. Numerical variables were statistically evaluated via Student's t-tests (*$p < 0.05$). **(F)** Immunofluorescence staining of ssHFGs generated using the PDMS oxy(+) **(i)** and PMMA oxy(−) **(ii)** chips. Blue, nuclei; green, HIF-1α. (For interpretation of the references to colour in this figure legend, the reader is referred to the web version of this article.)

To further confirm these results, we next placed the PDMS oxy(+) chip in a multigas incubator under controlled conditions of 2%, 10%, or 21% oxygen (Fig. S2A). The expression levels of versican and *HIF-1α* in cells grown under these conditions were positively and negatively correlated with increased oxygen supply, respectively (Fig. S2B), again suggesting that an adequate oxygen supply was required for the trichogenic functions exhibited by HFGs generated using the oxy(+) chip.

To date, the 'hanging drop' approach has been routinely used to generate spheroids and embroid bodies [21]. Therefore, in the present study, drops of culture medium containing 8×10^3 cells were placed on the lids of culture dishes, and the cells were subjected to hanging drop culture for 3 days (Fig. S3). Although this technique should facilitate sufficient supply of oxygen to the cultured cells, only small aggregates, and no ssHFGs, formed during the culture period. This likely reflected the fact that the volume of culture medium was dramatically limited in this culture method, potentially resulting in a shortage of nutrients and/or cytotoxic variations in the pH of the culture medium.

Taken together, these results suggested that PDMS was an optimal material for the fabrication of HFG chips capable of supporting the large-scale preparation of ssHFGs. Furthermore, we demonstrated that, due to the simplicity and scalability of the utilized fabrication processes and configurations, the PDMS HFG chip was suitable for expansion to comprise ~5000 microwells. Using this expanded chip, we were able to successfully prepare and collect ~5000 spherical aggregates (Fig. S4).

3.4. Transplantation of spatially aligned ssHFGs

ssHFGs were prepared in a dense and spatially regulated manner on the HFG chip. We hypothesized that their transplantation in this same arrangement may be both beneficial to and practical for human hair regeneration therapy. By considering the average number of hair shafts generated from single ssHFGs (Fig. 4C), a cell seeding density was chosen such that the prospective density of hair shafts would be roughly the same as that on the human head. A collagen solution, reinforced with an embedded surgical mesh to improve handling, was poured and set on the HFG chip after ssHFG formation (Fig. 7A). Successful transfer of the ssHFGs to the hydrogel layer was confirmed by their removal from the HFG chip when the hydrogel was peeled away (Fig. 7A(i, ii)). Since the back skin of nude mice represented a small and somewhat wrinkled transplantation area, the hydrogel sheet was cut into small pieces comprising ~10 ssHFGs in a column-arrangement, each of which was then transplanted into the nude mice (Fig. 1B). At 18 days after transplantation, a high density of hairs was observed at the transplantation sites (Fig. 7B), and the generated hair follicles were aligned in a straight line, as demonstrated by histochemical staining. Notably, the distance between the generated hair follicles was less than one-tenth that of the originally distance between ssHFGs located on the HFG chip (Fig. 7C). Although further studies are needed to confirm and clarify these observations, one potential explanation is that collagen shrinkage may have been induced after transplantation by any of a number of proteinases (including collagenase) known to function *in vivo* [41].
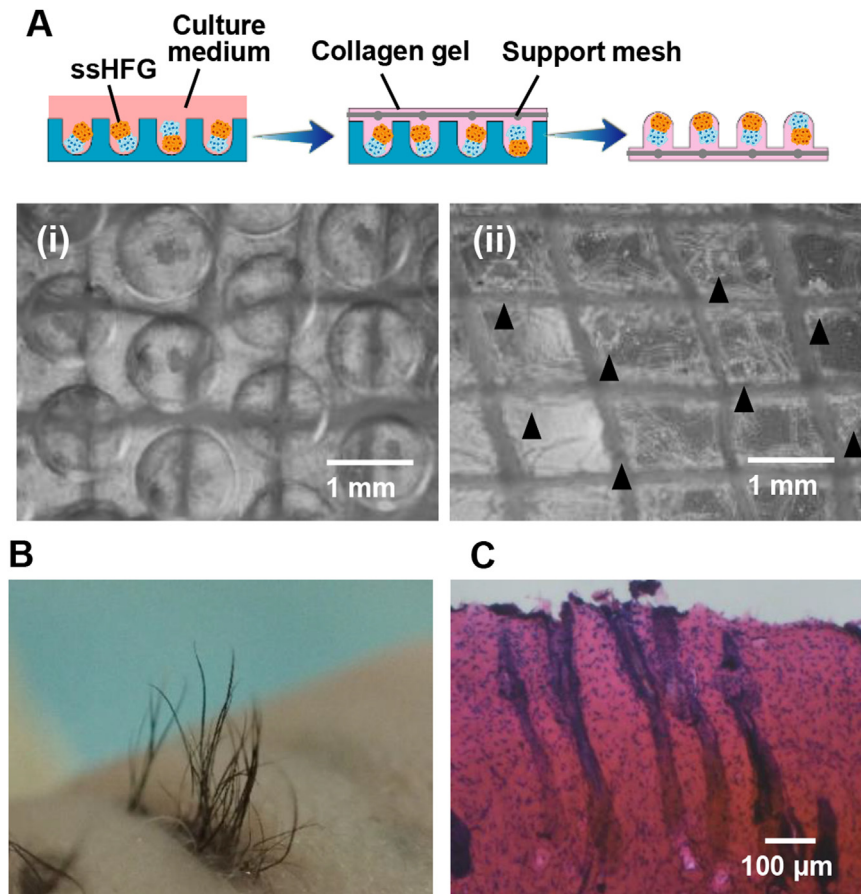
Fig. 7. Spatially aligned, simultaneous transplantation of ssHFGs. (A) Schematic representation showing the ssHFGs being embedded in a collagen gel to enable their transplantation. Representative photographs depict HFG appearance prior to **(i)** and after **(ii)** the collagen gel was removed from the HFG chip. Arrowheads indicate HFGs. **(B)** Generated hairs 18 days after the transplantation of collagen-embedded ssHFGs. **(C)** HE staining of cross-sections of the generated hair follicles. Epidermal layers were lost during sectioning of samples.

4. Conclusion

In the present study, we demonstrated the fabrication of a culture array chip for the large-scale preparation of ssHFGs via a two-step molding process. Seeding a mixture of dissociated epithelial and mesenchymal cells on this chip resulted in their self-organization to form aggregates and subsequent ssHFGs. The supply of adequate oxygen through the gas-permeable substrate used to fabricate the chip was demonstrated to be essential for the spontaneous self-organization of HFGs capable of generating hair shafts after transplantation into the back or scalp skin of nude mice. Regularly aligned hair follicles were generated by transferring ssHFGs from the chip via a collagen gel that enabled direct intracutaneous transplantation. Notably, the experiments conducted in the present study utilized murine cells, and thus, further studies of human trichogenic cells are required to assess the feasibility of this novel method for use in human hair-regenerative medicine. In fact, preliminary results generated in the present study showed that spontaneous cell separation and ssHFG formation could be achieved by seeding human keratinocytes and DP cells on the HFG chip. We hope to extend these preliminary analyses in the future in order to assess the suitability of this method to the culture of other potential human cell sources of both epithelial and dermal cell populations, such as bulge epithelial stem and keratinocyte precursor (epithelial) cells, as well as trichogenic dermal cells derived from stem or progenitor cells.

Appendix A. Supplementary data

Supplementary data related to this article can be found at https://doi.org/10.1016/j.biomaterials.2017.10.056.

References

[1] J.C. Vary, Selected disorders of skin appendages-acne, alopecia, hyperhidrosis, Med. Clin. North Am. 99 (2015) 1195–1211.
[2] N. Orentreich, Autografts in alopecias and other selected dermatological conditions, Ann. N.Y. Acad. Sci. 83 (1959) 463–479.
[3] S.B. Mahjour, F. Ghaffarpasand, H. Wang, Hair follicle regeneration in skin grafts: current concepts and future perspectives, Tissue Eng. Part B Rev. 18 (2012) 15–23.
[4] M.E. Balana, H.E. Charreau, G.J. Leiros, Epidermal stem cells and skin tissue engineering in hair follicle regeneration, World J. Stem Cells 7 (2015) 711–727.
[5] S.E. Millar, Molecular mechanisms regulating hair follicle development, J. Invest. Dermatol. 118 (2002) 216–225.
[6] M. Rendl, L. Lewis, E. Fuchs, Molecular dissection of mesenchymal-epithelial interactions in the hair follicle, PLos Biol. 3 (2005) 1910–1924.
[7] M. Ohyama, Y. Zheng, R. Paus, K.S. Stenn, The mesenchymal component of hair

follicle neogenesis: background, methods and molecular characterization, Exp. Dermatol. 19 (2010) 89—99.

[8] M. Ohyama, O. Veraitch, Strategies to enhance epithelial-mesenchymal interactions for human hair follicle bioengineering, J. Dermatol. Sci. 70 (2013) 78—87.

[9] C.A.B. Jahoda, K.A. Horne, R.F. Oliver, Induction of hair growth by implantation of cultured dermal papilla cells, Nature 311 (1984) 560—562.

[10] W.C. Weinberg, L.V. Goodman, C. George, D.L. Morgan, S. Ledbetter, S.H. Yuspa, U. Lichti, Reconstitution of hair follicle development in vivo: determination of follicle formation, hair growth, and hair quality by dermal cells, J. Invest. Dermatol. 100 (1993) 229—236.

[11] Y. Zheng, X.B. Du, W. Wang, M. Boucher, S. Parimoo, K.S. Stenn, Organogenesis from dissociated cells: generation of mature cycling hair follicles from skin-derived cells, J. Invest. Dermatol. 124 (2005) 867—876.

[12] R. Ehama, Y. Ishimatsu-Tsuji, S. Iriyama, R. Ideta, T. Soma, K. Yano, C. Kawasaki, S. Suzuki, Y. Shirakata, K. Hashimoto, J. Kishimoto, Hair follicle regeneration using grafted rodent and human cells, J. Invest. Dermatol. 127 (2007) 2106—2115.

[13] C.A. Higgins, J.C. Chen, J.E. Cerise, C.A. Jahoda, A.M. Christiano, Microenvironmental reprogramming by three-dimensional culture enables dermal papilla cells to induce de novo human hair-follicle growth, Proc. Natl. Acad. Sci. U. S. A. 110 (2013) 19679—19688.

[14] Y.C. Huang, C.C. Chan, W.T. Lin, H.Y. Chiu, R.Y. Tsai, T.H. Tsai, J.Y. Chan, S.J. Lin, Scalable production of controllable dermal papilla spheroids on PVA surfaces and the effects of spheroid size on hair follicle regeneration, Biomaterials 34 (2013) 442—451.

[15] Y. Miao, Y.B. Sun, B.C. Liu, J.D. Jiang, Z.Q. Hu, Controllable production of transplantable adult human high-passage dermal papilla spheroids using 3D Matrigel culture, Tissue Eng. Part A 20 (2014) 2329—2338.

[16] B. Lin, Y. Miao, J. Wang, Z. Fan, L. Du, Y. Su, B. Liu, Z. Hu, M. Xing, Surface tension guided hanging-drop: producing controllable 3D spheroid of high-passaged human dermal papilla cells and forming inductive microtissues for hair-follicle regeneration, ACS Appl. Mater. Interfaces 8 (2016) 5906—5916.

[17] C.M. Yen, C.C. Chan, S.J. Lin, High-throughput reconstitution of epithelial-mesenchymal interaction in folliculoid microtissues by biomaterial-facilitated self-assembly of dissociated heterotypic adult cells, Biomaterials 31 (2010) 4341—4352.

[18] K. Toyoshima, K. Asakawa, N. Ishibashi, H. Toki, M. Ogawa, T. Hasegawa, T. Irie, T. Tachikawa, A. Sato, A. Takeda, T. Tsuji, Fully functional hair follicle regeneration through the rearrangement of stem cells and their niches, Nat. Commun. 3 (2012).

[19] U. Lichti, J. Anders, S.H. Yuspa, Isolation and short-term culture of primary keratinocytes, hair follicle populations and dermal cells from newborn mice and keratinocytes from adult mice for in vitro analysis and for grafting to immunodeficient mice, Nat. Protoc. 3 (2008) 799—810.

[20] I.T. Hoffecker, H. Iwata, Manipulation of cell sorting within mesenchymal stromal cell-islet cell multicellular spheroids, Tissue Eng. Part A 20 (2014) 1643—1653.

[21] J.M. Kelm, M. Fussenegger, Microscale tissue engineering using gravity-enforced cell assembly, Trends Biotechnol. 22 (2004) 195—202.

[22] T. Anada, J. Fukuda, Y. Sai, O. Suzuki, An oxygen-permeable spheroid culture system for the prevention of central hypoxia and necrosis of spheroids, Biomaterials 33 (2012) 8430—8441.

[23] J. Kishimoto, R. Ehama, L. Wu, S. Jiang, N. Jiang, R.E. Burgeson, Selective activation of the versican promoter by epithelial-mesenchymal interactions during hair follicle development, Proc. Natl. Acad. Sci. U. S. A. 96 (1999) 7336—7341.

[24] A. Osada, T. Iwabuchi, J. Kishimoto, T.S. Hamazaki, H. Okochi, Long-term culture of mouse vibrissal dermal papilla cells and de novo hair follicle induction, Tissue Eng. 13 (2007) 975—982.

[25] R.J. Morris, Y.P. Liu, L. Marles, Z. Yang, C. Trempus, S. Li, J.S. Lin, J.A. Sawicki, G. Cotsarelis, Capturing and profiling adult hair follicle stem cells, Nat. Biotechnol. 22 (2004) 411—417.

[26] M. Yamao, M. Inamatsu, Y. Ogawa, H. Toki, T. Okada, K.E. Toyoshima, K. Yoshizato, Contact between dermal papilla cells and dermal sheath cells enhances the ability of DPCs to induce hair growth, J. Invest. Dermatol. 130 (2010) 2707—2718.

[27] H. Oshima, A. Rochat, C. Kedzia, K. Kobayashi, Y. Barrandon, Morphogenesis and renewal of hair follicles from adult multipotent stem cells, Cell 104 (2001) 233—245.

[28] M.S. Steinberg, M. Takeichi, Experimental specification of cell sorting, tissue spreading, and specific spatial patterning by quantitative differences in cadherin expression, Proc. Natl. Acad. Sci. U. S. A. 91 (1994) 206—209.

[29] R.A. Foty, M.S. Steinberg, The differential adhesion hypothesis: a direct evaluation, Dev. Biol. 278 (2005) 255—263.

[30] L.L. Wang, L.X. Xue, H.X. Yan, J. Li, Y.C. Lu, Effects of ROCK inhibitor, Y-27632, on adhesion and mobility in esophageal squamous cell cancer cells, Mol. Biol. Rep. 37 (2010) 1971—1977.

[31] M.S. Steinberg, Reconstruction of tissues by dissociated cells. Some morphogenetic tissue movements and the sorting out of embryonic cells may have a common explanation, Science 141 (1963) 401.

[32] Y. Sun, Q. Wang, Modeling and simulations of multicellular aggregate self-assembly in biofabrication using kinetic Monte Carlo methods, Soft Mater. 9 (2013) 2172—2186.

[33] F. Jimenez, J.M. Ruifernández, Distribution of human hair in follicular units, Dermatol. Surg. 25 (1999) 294—298.

[34] K.S. Stenn, R. Paus, Controls of hair follicle cycling, Physiol. Rev. 81 (2001) 449—494.

[35] K. Foitzik, G. Lindner, S. Mueller-Roever, M. Maurer, N. Botchkareva, V. Botchkarev, B. Handjiski, M. Metz, T. Hibino, T. Soma, G.P. Dotto, R. Paus, Control of murine hair follicle regression (catagen) by TGF-beta1 in vivo, FASEB J. 14 (2000) 752—760.

[36] V.A. Randall, F.J. Ebling, Seasonal changes in human hair growth, Br. J. Dermatol. 124 (1991) 146—151.

[37] J. Fukuda, A. Khademhosseini, J. Yeh, G. Eng, J. Cheng, O.C. Farokhzad, R. Langer, Micropatterned cell co-cultures using layer-by-layer deposition of extracellular matrix components, Biomaterials 27 (2006) 1479—1486.

[38] F. Evenou, T. Fujii, Y. Sakai, Spontaneous formation of highly functional three-dimensional multilayer from human hepatoma Hep G2 cells cultured on an oxygen-permeable polydimethylsiloxane membrane, Tissue Eng. Part C Methods 16 (2010) 311—318.

[39] A. Khademhosseini, C. Bettinger, J.M. Karp, J. Yeh, Y. Ling, J. Borenstein, J. Fukuda, R. Langer, Interplay of biomaterials and micro-scale technologies for advancing biomedical applications, J. Biomater. Sci. Polym. Ed. 17 (2006) 1221—1240.

[40] G.L. Wang, B.H. Jiang, E.A. Rue, G.L. Semenza, Hypoxia-inducible factor 1 is a basic-helix-loop-helix-PAS heterodimer regulated by cellular O2 tension, Proc. Natl. Acad. Sci. U. S. A. 92 (1995) 5510—5514.

[41] R. Parenteau-Bareil, R. Gauvin, F. Berthod, Collagen-based biomaterials for tissue engineering applications, Materials 3 (2010) 1863—1887.